

*In situ* cleaning of diagnostic first mirrors: an experimental comparison between plasma and laser cleaning in ITER-relevant conditions

This content has been downloaded from IOPscience. Please scroll down to see the full text.

2017 Nucl. Fusion 57 046014

(<http://iopscience.iop.org/0029-5515/57/4/046014>)

View [the table of contents for this issue](#), or go to the [journal homepage](#) for more

Download details:

IP Address: 131.175.67.27

This content was downloaded on 02/03/2017 at 16:23

Please note that [terms and conditions apply](#).

# *In situ* cleaning of diagnostic first mirrors: an experimental comparison between plasma and laser cleaning in ITER-relevant conditions

A. Maffini<sup>1</sup>, L. Moser<sup>2</sup>, L. Marot<sup>2</sup>, R. Steiner<sup>2</sup>, D. Dellasega<sup>1,3</sup>, A. Uccello<sup>3</sup>, E. Meyer<sup>2</sup> and M. Passoni<sup>1,3</sup>

<sup>1</sup> Department of Energy, Politecnico di Milano, Via Ponzio 34/3, 20133 Milano, Italy

<sup>2</sup> Department of Physics, University of Basel, Klingelbergstrasse 82, CH-4056, Basel, Switzerland

<sup>3</sup> Istituto di Fisica del Plasma 'P. Caldirola', CNR, via R. Cozzi 53, 20125 Milano, Italy

E-mail: [alessandro.maffini@polimi.it](mailto:alessandro.maffini@polimi.it)

Received 14 September 2016, revised 20 December 2016

Accepted for publication 27 January 2017

Published 2 March 2017



CrossMark

## Abstract

This paper presents an experimental comparison between the plasma cleaning and the laser cleaning techniques of diagnostic first mirrors (FMs). The re-deposition of contaminants sputtered from a tokamak first wall onto FMs could dramatically decrease their reflectance in an unacceptable way for the proper functioning of plasma diagnostic systems. Therefore, suitable *in situ* cleaning solutions will be required to recover the FMs reflectance in ITER. Currently, plasma cleaning and laser cleaning are considered the most promising solutions. In this work, a set of ITER-like rhodium mirrors contaminated with materials tailored to reproduce tokamak redeposits is employed to experimentally compare plasma and laser cleaning against different criteria (reflectance recovery, mirror integrity, time requirement). We show that the two techniques present different complementary features that can be exploited for the cleaning of ITER FMs. In particular, plasma cleaning ensures an excellent reflectance recovery in the case of compact contaminants, while laser cleaning is faster, gentler, and more effective in the case of porous contaminant. In addition, we demonstrate the potential benefits of a synergistic solution which combines plasma and laser cleaning to exploit the best features of each technique.

Keywords: first mirror, ITER, plasma cleaning, laser cleaning, optical plasma diagnostics, rhodium, reflectance

(Some figures may appear in colour only in the online journal)

## 1. Introduction

Metallic first mirrors (FMs) will be crucial components of optical plasma diagnostics in ITER and future fusion reactors [1]. Since they will directly face the plasma, FMs might be subjected to both plasma erosion and deposition of materials sputtered from the tokamak first wall. In particular,

the dramatic decrease of FM reflectance due to contaminant deposition could lead to a failure of the corresponding diagnostic system, with an ultimate impact on the reactor safety and operability [1, 2]. Although passive mitigation techniques (special optical ducts with baffles, shutters and gas puffing in front of the mirror, etc) are predicted to reduce the amount of material deposited on FMs, suitable *in situ* cleaning solutions will be required to properly recover the FMs reflectance in ITER.

The ideal features that a FMs cleaning technique should have can be summarized as follows [3]:



Original content from this work may be used under the terms of the [Creative Commons Attribution 3.0 licence](https://creativecommons.org/licenses/by/3.0/). Any further distribution of this work must maintain attribution to the author(s) and the title of the work, journal citation and DOI.

- Safe for the mirror integrity (also in case of repeated treatments).
- Effective for different kinds of contaminants.
- Capable of situ treatment.
- Compatible with reactor environment (radiation, magnetic fields, etc).
- Fast and scalable to large areas (tens to hundreds of cm<sup>2</sup>).

Currently, the two most investigated solutions are plasma cleaning [4–10] and laser cleaning [11–17], both of which may have potential advantages and drawbacks.

In plasma cleaning, the contaminant material is removed thanks to physical sputtering by plasma ions. Plasma cleaning could be implemented in different forms, typically involving a local plasma generated by a direct current (DC) or by a radio-frequency (RF) discharge. The physics of plasma cleaning process is relatively straightforward. Since the cleaning action is achieved through binary collisions between the plasma ions and contaminants atoms, the plasma cleaning process takes place at the solid–plasma interface. For this reason, the cleaning time should in principle grow linearly with the deposit thickness. The sputtering rate generally increases with the ion energy, and also depends on the mass and binding energy of the target atoms. In the case of multi-elemental contaminants, the preferential sputtering of certain elements over others can change the composition of the contaminant material during the process. If the sputtering yield of the mirror itself is comparable with that of the contaminant, it becomes essential to avoid unnecessary mirror exposure to the cleaning plasma. This last requirement might be very challenging in the case of deposits characterized by strong non-homogeneity, either in terms of thickness or morphology.

In recent years, various experimental works involving RF plasma cleaning have shown promising results in terms of cleaning effectiveness and recovery of optical properties of mirrors contaminated with various fusion-relevant materials. Currently, RF plasma is the most studied solution for the cleaning of ITER FMs [18, 19].

In laser cleaning, pulsed laser radiation is exploited to remove the contaminant material through different processes, e.g. direct vaporization or thermomechanical delamination, sometimes taking place concurrently.

The physics behind laser cleaning process can be very complex because of a non-trivial interplay between optical phenomena (light absorption in contaminant and substrate, reflection at the interfaces, etc), heat transfer, and chemical/structural modifications possibly induced in both contaminant and substrate, that altogether make this process inherently nonlinear. Absorption of laser energy is a volume rather than surface phenomenon; therefore, it is less influenced by morphological properties. Laser ablation and laser damaging are threshold phenomena: depending on the laser parameters and material properties, it is possible to conceive a situation in which the contaminant is ablated without any modification to the substrate.

Today, laser cleaning is employed in highly-specialized applications (e.g. conservation of cultural heritage and micro-electronics) which require a remotely-operated, solvent-free cleaning process [20]. These features, along with its

versatility, make this technique a very appealing possibility for FMs cleaning. In the field of nuclear fusion, laser cleaning has been exploited to detritiate plasma facing components [21] and to clean optical windows [22].

However, the application of this technique to the cleaning of FMs is so far limited to a few experimental investigations [11, 14].

In previous works, we separately studied plasma cleaning [8–10] and laser cleaning [15–17] of mirrors in different experimental conditions.

In this paper, we provide a direct experimental comparison between plasma and laser cleaning techniques, in conditions that are potentially relevant to simulate the cleaning of ITER FMs. In addition, we explored the possibility of a synergistic approach in which laser and plasma cleaning techniques are combined to recover at best the original mirror properties.

In particular, a set of ITER-like rhodium (Rh) coated mirrors [23–26] was contaminated with laboratory-made tungsten/oxygen (W/O) and aluminum/tungsten/oxygen (Al/W/O, where Al is employed as beryllium proxy) compounds with different morphologies (from compact to porous), aimed to reproduce some of the features of the deposits that are expected on ITER FMs [26, 27] (section 2).

For each kind of contaminant, one mirror was plasma-cleaned with an argon plasma coupled with a RF source (section 3) and an exact replica was laser-cleaned with a nano-second laser system (section 4).

The results of the cleaning experiments were primarily evaluated by reflectance measurements. The mirrors' surface was also analyzed before and after the cleaning process, in order to identify possible damage sites and residual contaminants which hinder the recovery of pristine reflectance. Plasma and laser cleaning techniques were also compared in terms of the time required to perform the cleaning process (section 5).

The insights gathered from the direct comparison of the techniques allowed us to develop a combined cleaning strategy that foresees a laser cleaning treatment followed by a plasma cleaning session. This combined strategy ensured a complete recovery of specular reflectance without any detectable damage of the mirrors' surface.

## 2. Sample preparation and characterization

The mirrors used to perform the cleaning tests were Rh coatings (thickness ~ 500 nm) deposited on polished 316-L stainless steel (diameter 2.5 cm) by magnetron sputtering (MS) at Basel University.

Metallic coated mirrors with nanometer-sized crystallites are characterized by homogeneous sputtering upon plasma exposure and reduced technological issues if compared with single crystal mirrors. In particular, Rh coated mirrors are considered among the most interesting solution for the realization of ITER FMs, and were tested in different tokamak exposure campaigns (see [28] and references therein).

Even though other solutions for the production of Rh mirrors may be of interest [28, 29], we choose to work with MS Rh mirrors because they were exposed in the past to JET

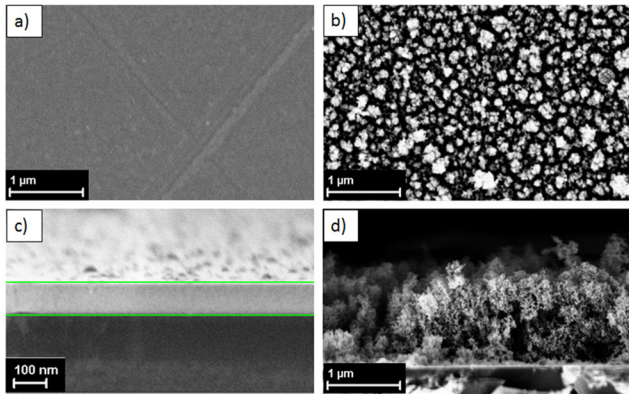


**Figure 1.** SEM micrographs of the W/O contaminants. (a) and (c) plane view and cross section of compact W/O (b) and (d) plane view and cross section of porous W/O.

plasma during different experimental campaigns [25, 26]. The process of MS deposition of Rh coatings is described in details in [23, 24].

Total, diffuse and specular reflectance ( $R_{\text{tot}}$ ,  $R_{\text{diff}}$  and  $R_{\text{spec}}$ , respectively) of each mirror was measured either with a Varian Cary 5 UV–vis–NIR spectrophotometer (incidence angle  $3^{\circ}20'$ ) or with a Perkin Elmer Lambda 1050 UV–vis–NIR spectrophotometer (incidence angle  $8^{\circ}$ ) in the 250–1800 nm wavelength range, of interest for most of the ITER optical diagnostics. In general, reflectance spectra of every Rh coating are very similar to each other and to handbook Rh reflectivity [30]. The typical specular reflectance of some pristine mirrors is shown as the solid black line (I) in figures 5, 9, 11, 13, and 17.

In order to reproduce the re-deposits that could build up in ITER and future reactors, the mirrors were contaminated by laboratory-made contaminants using the pulsed laser deposition (PLD) technique at Politecnico di Milano. In previous works, we exploited the PLD technique to deposit carbon-based and tungsten-based contaminants on thin film Rh mirrors in order to study and develop the laser cleaning of metallic FMs [15–17].

Here, we consider two classes of contaminants: binary tungsten-based W/O compounds and ternary aluminum-based Al/W/O compounds. Tungsten is the material of the ITER divertor and is also the reference material for the first wall of DEMO. Following the results of the mirror exposure campaign in ASDEX-UG [27], we employed W/O contaminants having a stoichiometry close to  $\text{WO}_3$ . Ternary Al/W/O contaminants are based upon the co-deposits found on the test mirrors exposed in the JET-ILW divertor [26]. Such co-deposits were mainly composed of beryllium (Be) and O, while the atomic ratio between Be and W was around 1% [26]. In this work, aluminum (Al) is chosen in substitution of Be—which will be the main constituent of ITER main chamber—because Be toxicity prevents this element from being easily adopted in ordinary, lab-scale facilities. Be and Al have similar electronegativity and form very stable and hard oxides; in addition, both elements are known to form alloys with W. Al is therefore regarded as one of the best choices in order to mimic tokamak redeposits containing Be [31].

For each class of materials, two very different morphologies were considered: compact films and porous deposits.

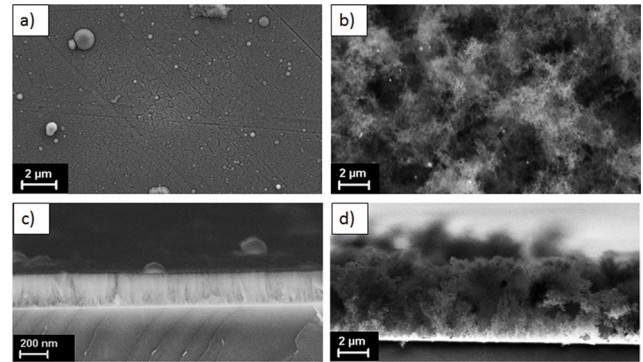


**Figure 2.** SEM micrographs of the Al/W/O contaminants. (a) and (c) plane view and cross section of compact Al/W/O (b) and (d) plane view and cross section of porous Al/W/O.

These two morphologies can be considered representative of the wide variety of re-deposits that can be expected in different regions of a tokamak reactor under different operative conditions [26, 27, 32].

To summarize, 4 types of contaminants were investigated: compact W/O, porous W/O, compact Al/W/O and porous Al/W/O. Thanks to PLD versatility, their properties were finely controlled by adjusting the deposition parameters (such as laser wavelength, laser fluence, background pressure, and target composition [33]) in order to reproduce realistic tokamak-like deposits. In our previous works [17, 34], we have shown that PLD-made contaminants are suited to mimic the characteristics of the deposits found on test mirrors exposed in ASDEX-UG and JET-ILW in terms of composition, thickness, morphology and optical properties.

The PLD set-up was equipped with a Q-switched Nd:YAG Continuum II Powerlite laser (pulse duration 5–8 ns, repetition rate 10 Hz) with tunable wavelength ( $\lambda = 1064, 532$  and 266 nm). Laser pulses were focused on a rotating target made of a 99.99% purity W disk in the case of W/O contaminants, and on a 99.99% purity Al disk decorated with W wires (wire diameter 0.3 mm, area coverage 5.5 %) in the case of Al/W/O contaminants. W/O contaminants were produced with  $\lambda = 532$  nm and fluence per pulse of  $2.2 \text{ J cm}^{-2}$ . Al/W/O contaminants were produced with  $\lambda = 1064$  nm and  $4.3 \text{ J cm}^{-2}$ . For both compounds, the morphology was controlled by acting on the deposition atmosphere. Compact deposits were obtained with 5 Pa  $\text{O}_2$ , porous deposits with 100 Pa Ar. Further details about PLD of W/O and Al/W/O contaminants can be found in [17, 34].

Two identical samples were prepared for each type of contaminant, one to be plasma cleaned and the other to be laser cleaned. Each replica was deposited in exactly the same conditions of the other one.

The mirrors' surface morphology after contaminant deposition was assessed by scanning electron microscopy (SEM) with a Zeiss Supra 40 SEM. Examples of W/O and Al/W/O contaminant morphology are reported in figures 1 and 2. Compact W/O films (figures 1(a) and (c)) showed a smooth, featureless surface. The mean thickness was about 100 nm. Porous W/O films (figures 1(b) and (d)) were characterized by a low density



**Table 1.** Deposition parameters and properties of the contaminants employed in the mirror cleaning experiments. For each kind of contamination, two replicas were produced.

Contaminant	Deposition parameters			Contaminant properties	
	Wavelength (nm)	Fluence ( $\text{J cm}^{-2}$ )	Background gas	Avg. thickness (nm)	Composition
Compact W/O	532	2.2	O <sub>2</sub> , 5 Pa	100	O/W = 2.8
Porous W/O	532	2.2	Ar, 100 Pa	1000	O/W = 2.9
Compact Al/W/O	1064	4.3	O <sub>2</sub> , 5 Pa	250	O/Al = 2.2 W = 0.7 at. %
Porous Al/W/O	1064	4.3	Ar, 100 Pa	2000	O/Al = 2.2 W = 0.6 at. %

foam-like structure. The average thickness was 1  $\mu\text{m}$ . Compact Al/W/O films (mean thickness of about 250 nm) showed a relatively flat surface with some micrometric droplets and sub-micrometric cracks (figures 2(a) and (c)). The morphology of porous Al/W/O (figures 2(b) and (d)) was characterized by a very open structure with a significant amount of voids. In this case the average thickness was about 2.5  $\mu\text{m}$ .

Elemental composition of the deposits was checked by energy dispersive x-ray spectroscopy (EDXS, accelerating voltage 5–7 kV). Additional information about chemical and structural properties of the samples was obtained with Raman spectroscopy (Renishaw InVia Raman spectrometer using the 514.5 nm wavelength of an Ar<sup>+</sup> laser) and x-ray photoelectron spectroscopy (XPS). A description of XPS setup as well as peak fitting procedure are given in [35].

Considering the W/O contaminants, EDXS analysis gave an O/W atomic ratio  $\approx 2.8$ , close to that of WO<sub>3</sub>. Raman analysis (not shown) confirms that W/O contaminants were made of amorphous tungsten tri-oxides with some stoichiometric defects (oxygen vacancies) [17].

In the case of Al/W/O samples, the elemental composition of O/Al atomic ratio was  $\approx 2.1$ , while W fraction was around 0.7 at.%. Raman analysis (not shown) did not reveal any defined peak in the 100–1300  $\text{cm}^{-1}$  range, indicating the amorphous structure of the samples [34]. XPS analysis of the Al 2p and W 4f peaks (not shown) showed a complete oxidation of both Al (in the form of Al<sub>2</sub>O<sub>3</sub>) and W (as WO<sub>3</sub>).

In table 1 we summarize the properties of the 4 types of samples used in the cleaning experiments, together with their deposition parameters. The reflectance (total, diffuse and specular) of contaminated mirrors was measured with the Varian Cary 5 and Perkin Elmer Lambda 1050 spectrophotometers in the 250–1800 nm wavelength range. Specular reflectance of the contaminated mirrors (red line, II, dashed) is shown in figure 5(a) (compact W/O), figure 5(b) (porous W/O), figure 9(a) (compact Al/W/O) and figure 9(b) (porous Al/W/O), respectively.

### 3. Plasma cleaning results

#### 3.1. Plasma cleaning procedure and plasma exposure damage test

A schematic of the plasma exposure facility exploited to perform the plasma cleaning experiments is shown in [36]. The mirror to be cleaned was capacitively coupled to a radio

frequency (13.56 MHz) power supply, while the vacuum chamber acted as the grounded electrode. The vacuum chamber was filled with 0.5 Pa of Ar, which worked as sputter gas. Because of the alternate positive and negative potential applied to the electrode with RF, even insulating contaminants (as for both W/O and Al/W/O) do not charge up with time and can be sputtered by ions. Moreover, due to the smaller mass of electrons compared to ions, more negative charges are collected on the electrode during a period giving rise to a negative DC component called self-bias. The latter determines the energy of the Ar<sup>+</sup> ions responsible for the sputtering of the contaminant.

The choice of Ar<sup>+</sup> energy is a tradeoff between time requirements and the necessity of preserving mirror integrity. In our previous works, we observed that an energy around 300 eV ensured a sufficient sputtering yield and was not detrimental for the mirror surface quality [9].

Therefore, the power delivered by the RF generator during the cleaning experiments was automatically regulated to have a self-bias of  $-300$  V. Since the plasma potential was in the order of 27–30 V, the resulting energy of the Ar<sup>+</sup> ions impinging on the samples was around 330 eV. The Ar<sup>+</sup> flux on the samples was approximately  $2 \times 10^{18} \text{ m}^{-2} \text{ s}^{-1}$ .

In order to keep track of the plasma cleaning process, the evolution of the mirror relative reflectance (i.e. the ratio of the actual reflectance at a given time to the reflectance at the beginning of the plasma exposure) was continuously monitored with an *in situ* reflectometry set-up in the 400–800 nm wavelength range. The light emitted by a fiber-coupled halogen lamp was split in two beams, one focused on the sample with an incidence angle of 45° (probe) and the other directed toward an AVANTES USB spectrometer. The latter works as a reference to correct for the lamp intensity variations. The light reflected from the sample is collected using an integrating sphere coupled to a second spectrometer, identical to the first one. By measuring the ratio between the signal and the reference value it is possible to deduce the relative variation of the sample's reflectance. Further details about the *in situ* spectrophotometry can be found in [36].

Typically, the plasma treatment was maintained as long as a reflectance increase was appreciable. Then, when the reflectance reached a plateau and eventually started to slowly decrease, the plasma was turned off to avoid unnecessary plasma exposure. In some cases, plasma cleaning treatments were also occasionally suspended to perform *in situ* XPS or *ex situ* absolute reflectance measurements.

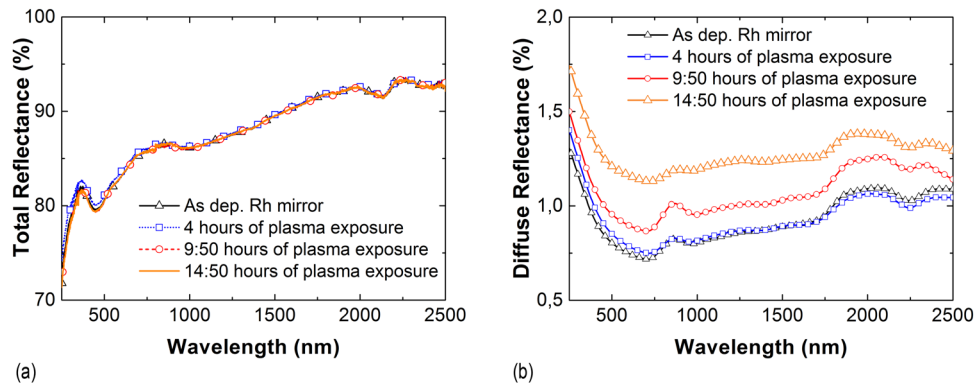


**Figure 3.** (a)  $R_{\text{tot}}$  of a Rh mirror before plasma exposure (black triangles), after 4 h of plasma treatment (blue squares), after 9.5 h of plasma treatment (red circles), and after 14.5 h of plasma treatment (solid orange). (b)  $R_{\text{diff}}$  of a Rh mirror before plasma exposure (black triangles), after 4 h of plasma treatment (blue squares), after 9.5 h of plasma treatment (red circles), and after 14.5 h of plasma treatment (solid orange).

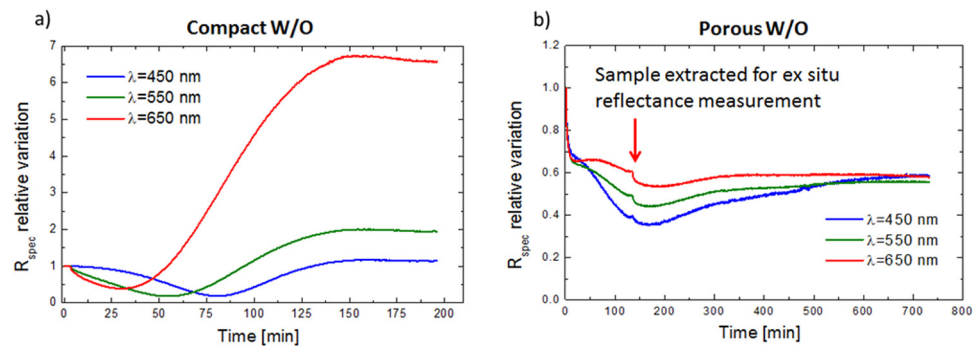


**Figure 4.** Evolution of relative specular reflectance as a function of accumulated plasma exposure time for: (a) mirror contaminated with compact W/O (b) mirror contaminated with porous W/O. Relative  $R_{\text{spec}}$  is evaluated at  $\lambda = 450$  nm (blue line),  $\lambda = 550$  nm (green line), and  $\lambda = 650$  nm (red line). An arrow marks the point when the porous W/O sample was extracted from the chamber for an absolute measurement of its reflectance.

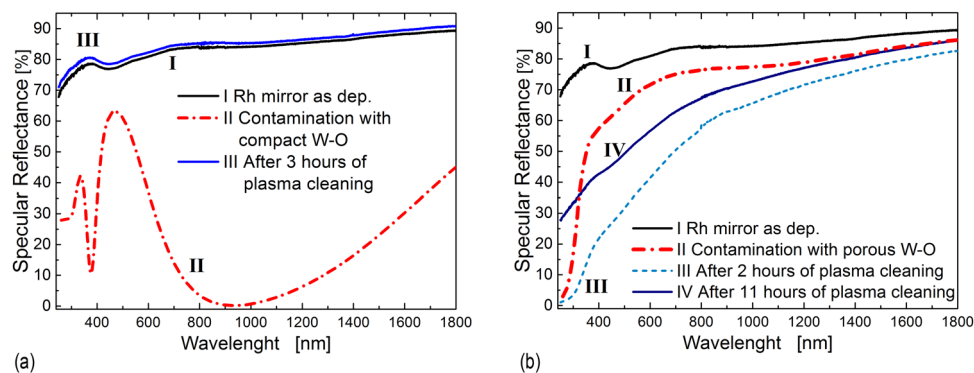


**Figure 5.** (a)  $R_{\text{spec}}$  of a Rh mirror before contamination (I, solid black), contaminated with compact W/O (II, dashed red) and after 3 h of plasma cleaning (III, solid blue). (b)  $R_{\text{spec}}$  of a Rh mirror before contamination (I, solid black), contaminated with porous W/O (II, dashed red), after 2 h of plasma cleaning (III, dashed light blue), and after 11 h of plasma cleaning (IV, solid dark blue).

In order to understand the effects of plasma exposure on the mirror properties, a bare Rh mirror was exposed to the same plasma conditions used for the cleaning experiments ( $\text{Ar}^+$  energy = 330 eV, flux =  $2 \times 10^{18} \text{ m}^{-2} \text{ s}^{-1}$ ). Total and diffuse reflectance were measured *ex situ* after 1 h, 4 h, 9.5 h and 14.5 h of plasma exposure. Because of the  $\text{Ar}^+$  sputtering, the Rh coating thickness was reduced from  $\approx 600$  nm (initial value) to a minimum of  $\approx 170$  nm (14.5 h). In addition, the average arithmetic roughness parameter  $R_a$  increased from 30.1 nm to 41.8 nm. Apart from these modifications, no macroscopic or microscopic damages were observed. Total and diffuse reflectance of the

exposed mirror are shown in figures 3(a) and (b), respectively. By comparing the black lines (initial value) with the orange lines (14.5 h of plasma exposure), it is possible to conclude that the effects of the plasma treatment are not detrimental to the optical properties of an uncontaminated Rh-coated mirror.

### 3.2. Plasma cleaning of W/O contaminated mirrors

The time evolution of relative  $R_{\text{spec}}$  for the mirror contaminated with compact W/O during the cleaning is shown in figure 4(a). For this kind of contamination, the reflectance in

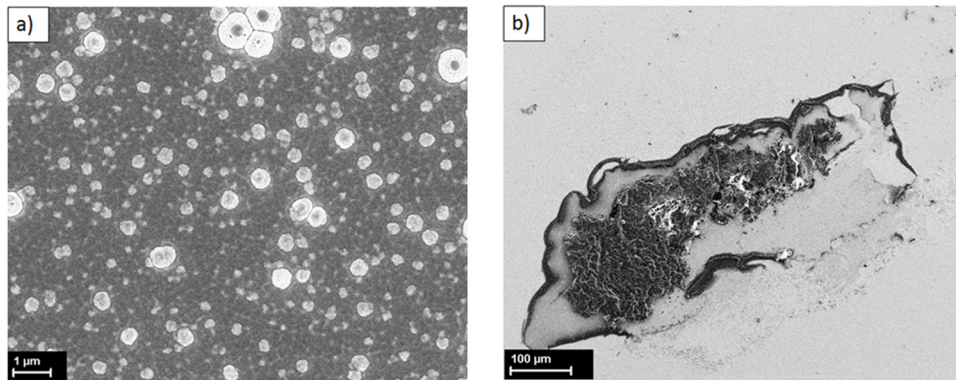


**Figure 6.** SEM top-view of the mirror contaminated with porous W/O after 12h of plasma cleaning treatment. (a) High magnification image of W/O residuals, taken from a region without macroscopic damages. (b) Low magnification image of the millimetric-wide damage site.

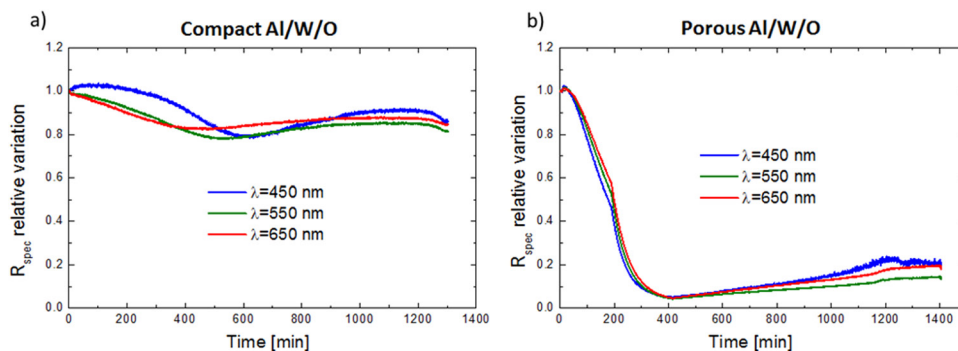


**Figure 7.** Evolution of relative specular reflectance as a function of accumulated plasma exposure time for mirrors contaminated with: (a) compact Al/W/O, (b) porous Al/W/O. Relative  $R_{\text{spec}}$  is evaluated at  $\lambda = 450$  nm (blue line),  $\lambda = 550$  nm (green line), and  $\lambda = 650$  nm (red line).

the visible region was determined by thin film interference effects, as can be seen from figure 5(a) (dashed red line, II). As the plasma sputtering started to reduce the thickness of the W/O layer, the spectral positions of the reflectance maxima and minima were shifted towards shorter wavelengths. The reflectance at a certain wavelength varied correspondingly. This behavior is clearly appreciable in figure 4(a), observing that for each wavelength the reflectance has a minimum corresponding to the thickness at which destructive interference occurs. After 3 h of plasma exposure, the relative reflectance reached a stable plateau, and therefore the cleaning was stopped. SEM and XPS analyses highlighted that the mirror surface was completely free from contaminant residuals (not shown). The original  $R_{\text{spec}}$  was fully recovered, as shown in figure 5(a) (solid blue line, III).

The relative  $R_{\text{spec}}$  evolution for the mirror contaminated with porous W/O followed a completely different behavior (figure 4(b)). A prompt drop in relative reflectance is observed in correspondence to the beginning of plasma treatment. About 30% of the initial reflectance was lost in a few minutes, then  $R_{\text{spec}}$  decreased with an almost constant rate. The treatment was interrupted after 2 h, and the surface composition was checked by XPS. W (total 40 at.%), O (29 at.%) and Rh (31 at.%) were detected. The W4f core level spectrum was deconvoluted in metallic (24 at.%),  $\text{WO}_2$  (7.5 at.%) and  $\text{WO}_3$  (8.5 at.%) component, thus suggesting that the plasma cleaning process reduced the oxygen content of W/O contaminant probably because O is more easily sputtered than W.

Oxygen depletion can have modified the optical properties of the  $\text{WO}_3$  open nanostructures, explaining the prompt drop in relative reflectance experienced by the mirror as soon as the plasma treatment started (figure 4(b)).

The sample was then taken out from the chamber and its absolute  $R_{\text{spec}}$  was measured (figure 5(b), dashed light blue line, III). Since the reflectance was unacceptably low, the mirror was loaded again in the chamber for additional 10 h of plasma cleaning treatment. Also in this occasion, reflectance dropped suddenly as the plasma was turned on. The specular reflectance after 12 h of plasma cleaning is shown in figure 5(b), solid dark blue line (IV). The reflectance recovery is not satisfactory, especially in the UV–vis region.

A SEM micrograph of the mirror surface after the cleaning treatment (12 h) is reported in figure 6. Globular-shaped residuals can be seen in figure 6(a). In figure 6(b), it is possible to appreciate a millimetric region where the Rh coating was severely damaged by the prolonged plasma exposure.

### 3.3. Plasma cleaning of Al/W/O contaminated mirrors

The relative  $R_{\text{spec}}$  variation of the mirror contaminated with compact Al/W/O as a function of plasma exposure time is shown in figure 7(a). As discussed for compact W/O contamination, the evolution of relative reflectance was driven by interference phenomena as long as the thickness of the Al/W/O coating was decreasing because of the plasma sputtering. Then, after about 20 h of plasma exposure, the reflectance



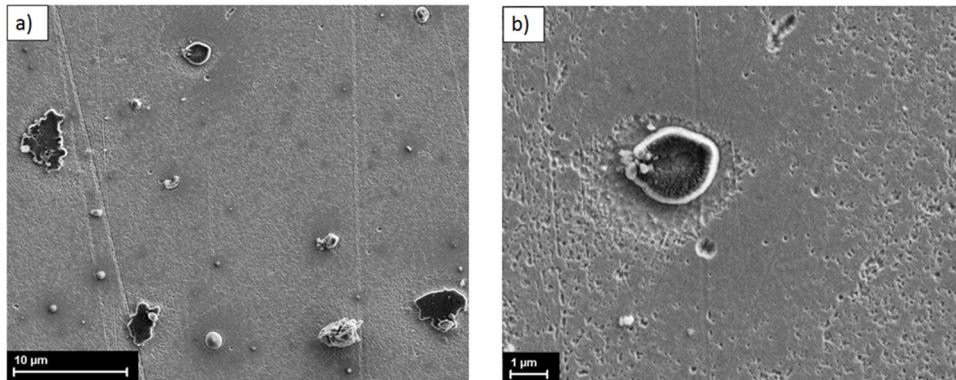


**Figure 8.** SEM top-view of the mirror contaminated with compact Al/W/O after 21 h of plasma cleaning treatment. (a) Al/W/O residuals (b) surface modifications induced by plasma exposure.

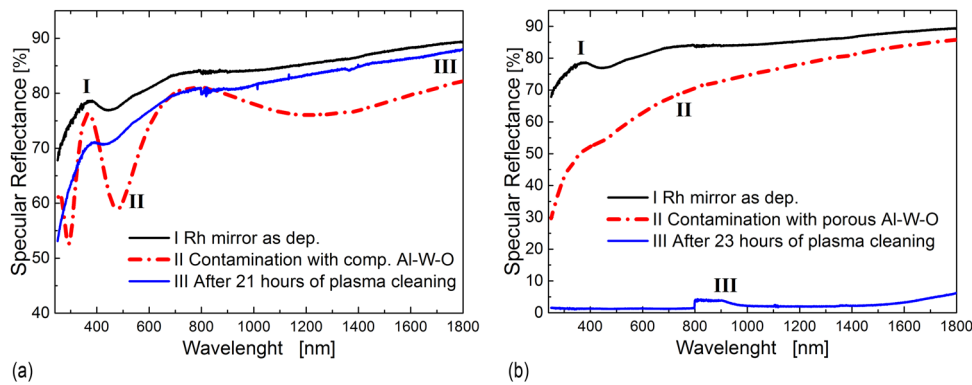


**Figure 9.** (a)  $R_{\text{spec}}$  of a Rh mirror before contamination (I, solid black), contaminated with compact Al/W/O (II, dashed red) and after 21 h of plasma cleaning (III, solid blue). (b)  $R_{\text{spec}}$  of a Rh mirror before contamination (I, solid black), contaminated with porous Al/W/O (II, dashed red) and after 23.5 h of plasma cleaning (III, solid blue).

started to decrease simultaneously for the 3 wavelengths. We interpreted it as a signal of possible mirror damaging, and therefore the cleaning was halted. The plasma exposure for this sample lasted 21 h.

As appears from SEM micrograph in figure 8(a), some micrometric fragments of the Al/W/O contaminant layer were still present on the mirror surface after the cleaning treatment. Besides these fragments, the surface appeared on the whole free from residuals. XPS surface analysis detected a small amount of Al (18 at.%) together with O (36 at.%) and Rh (46 at.%). From figure 8(b) it is also possible to notice that the Rh coating has become pockmarked as a consequence of the plasma exposure.

The plasma cleaning treatment ensured a satisfactory  $R_{\text{spec}}$  recovery, as shown by the absolute reflectance measurement reported in figure 9(a). The missing  $R_{\text{spec}}$  is caused by both a decrease in  $R_{\text{tot}}$  and ( $\sim 9\%$  at  $\lambda = 250$  nm, not shown) and an increase in  $R_{\text{diff}}$  ( $\sim 6\%$  at  $\lambda = 250$  nm, not shown).

*In situ* relative reflectance evolution for porous Al/W/O contamination is shown in figure 7(b).  $R_{\text{spec}}$  steadily decreased during the plasma treatment, being almost completely lost after 7 h of plasma exposure. The plasma process was run for a total of 23.5 h, when  $R_{\text{spec}}$  was about one fifth of the original value. As confirmed by absolute  $R_{\text{spec}}$  measurement (figure 9(b)), the specular reflectance was dramatically lost as a consequence of the plasma cleaning. SEM and EDXS analyses showed that the Rh coating was completely destroyed in

several regions of the sample surface. An example is given in the SEM micrograph reported in figure 10(a), where the stainless steel (SS) substrate is visible. It is evident that the selected cleaning parameters (i.e. ion mass and energy) are not compatible with this combination of mirror and contaminant. Apart from the steel substrate, which preserved its smoothness, the remaining material presents the peculiar morphology shown in figure 10(b). XPS analysis revealed that it was composed of only Rh and O. Since it was not possible to detect Al signal, it can be deduced that most of the contaminant has been removed by the plasma treatment. We speculate that plasma ions have started to sputter (and eventually destroy) the Rh coating while—in other regions of the sample—contaminants were still present. Further investigations are required to understand the nature of such peculiar structures and the processes that lead to their formation.

## 4. Laser cleaning results

### 4.1. Laser cleaning procedure and laser damage test

Laser cleaning was performed in high-vacuum ( $10^{-3}$  Pa) to avoid oxidation and to consider realistic conditions in view of tokamak application. The laser cleaning experiments were performed using the fourth harmonic ( $\lambda = 266$  nm) of the Q-switched Nd:YAG laser employed to produce mirrors' contaminants (see section 2). The laser beam hits the sample at



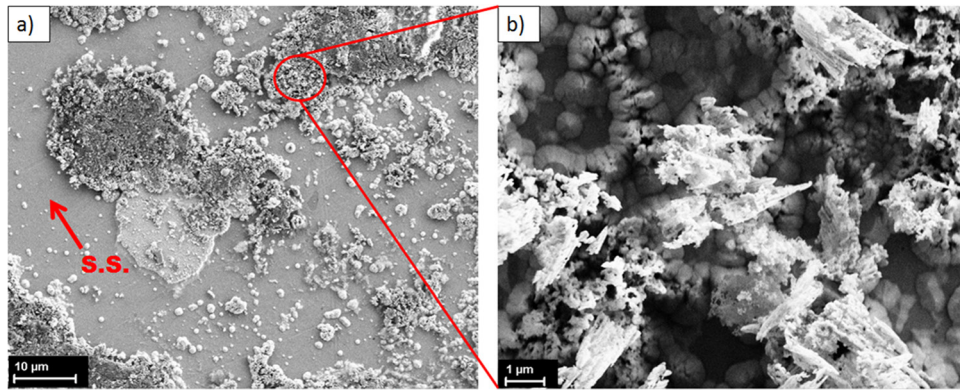


**Figure 10.** SEM top-view of the mirror contaminated with porous Al/W/O after 23.5 h of plasma exposure treatment. (a) Overview showing different residuals and SS substrate, (b) close up on the residuals.

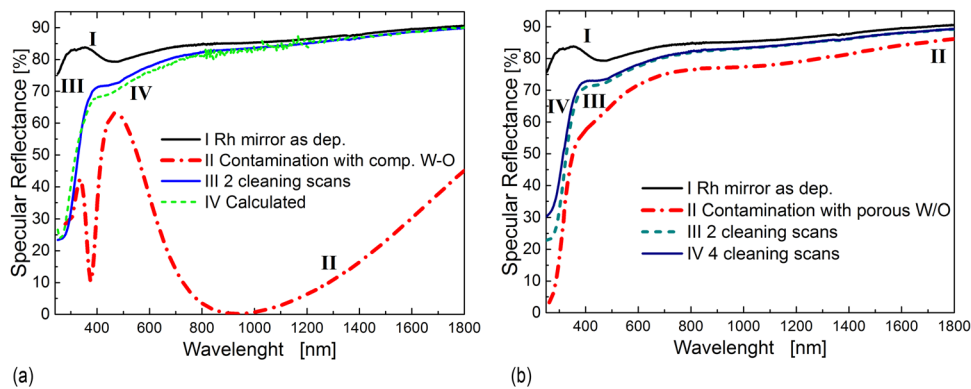


**Figure 11.** (a)  $R_{\text{spec}}$  of a Rh mirror before contamination (I, solid black), contaminated with compact W/O (II, dashed red) and after 2 laser cleaning scans (III, solid blue). The dashed green line (IV) shows the reflectance calculated by supposing a 5 nm thick WO<sub>3</sub> film (Cauchy layer with  $n = 2.17$  at  $\lambda = 550$  nm) on top of the Rh film. (b)  $R_{\text{spec}}$  of a Rh mirror before contamination (I, solid black), contaminated with porous W/O (II, dashed red), after 2 laser cleaning scans (III, dashed light blue) and after 4 laser cleaning scans (IV, solid dark blue).

45° and the laser spot on the sample has an elliptical shape with the major axis equal to 12.7 mm and minor axis to 9 mm.

With the aim of cleaning areas of some cm<sup>2</sup> ensuring a uniform irradiation of the sample, the latter was moved during the cleaning treatment with the sample handling routine described in [16]. As a result, the laser beam traced multiple vertical stripes on the sample surface, with a partial overlap in the horizontal direction between two adjacent stripes. A whole laser scan of the mirror surface takes around 1 min to be completed. Taking into account the partial overlapping of consecutive pulses in the same stripe and in the adjacent ones, each point of the irradiated surface receives, on the average, 45 pulses per scan. If necessary, multiple scans can be repeated seeking for an improvement of contaminant removal. More details about the laser cleaning procedure can be found in [16, 17].

Preliminary laser damage tests were performed on bare Rh mirrors to find a range of laser fluence values safe for mirror integrity. The presence of damages was checked by both careful visual inspection and SEM microscopy. We found that sub-millimetric delamination of a bare magnetron sputtered Rh coating starts to develop after a single scan with a fluence per pulse equal to 110 mJ cm<sup>-2</sup>. Employing a fluence per pulse of 70 mJ cm<sup>-2</sup> no damages were observed, even in case of 4 consecutive scans. Therefore, the laser cleaning experiments described in the following were performed with

a fluence of 70 mJ cm<sup>-2</sup> per pulse. As a general consideration, it is worth to note that the laser damage threshold for a film-coated mirror can depend significantly on the coating deposition method and on the substrate properties as well. For example, we measured a laser damage threshold higher than 150 mJ cm<sup>-2</sup> for 1 μm thick Rh films produced by PLD [16].

Mirrors' reflectance ( $R_{\text{tot}}$ ,  $R_{\text{diff}}$  and  $R_{\text{spec}}$ ) was recorded after cleaning using the Perkin Elmer spectrophotometer. Cleaned mirrors were also characterized by SEM, EDXS and XPS.

#### 4.2. Laser cleaning of W/O contaminated mirrors

In figure 11(a) we report the specular reflectance of a pristine Rh mirror (solid black line, I), of a Rh mirror contaminated with compact W/O (dashed red line, II) and of the same mirror after 2 laser cleaning scans (solid light blue line, III) are reported in figure 11(a).

Owing to the laser cleaning treatment,  $R_{\text{spec}}$  was well recovered in the NIR–vis region (>90% of the pristine value). For  $\lambda < 400$  nm, however, a sharp drop in  $R_{\text{spec}}$  is evident. This threshold wavelength corresponds to the optical band-gap of W/O contaminants, as can be estimated from dashed red lines in figures 11(a) and (b), which describe the specular reflectance of contaminated mirrors before the cleaning treatment (the optical band gap of crystalline WO<sub>3</sub> is about 2.8 eV,

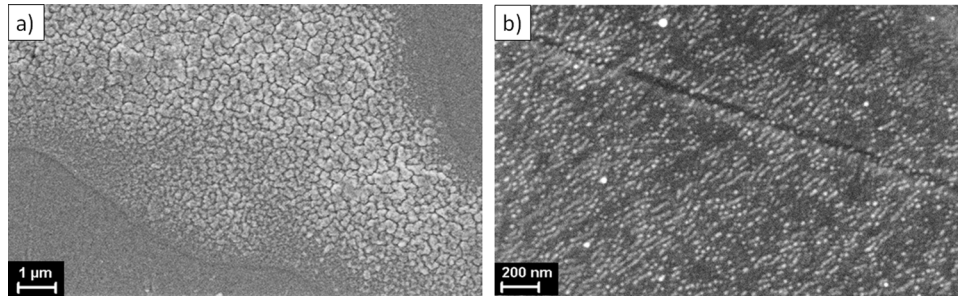


**Figure 12.** SEM top-view of: (a) compact W/O residuals after 2 laser cleaning scans, showing a peculiar, corrugated morphology (b) rod-shaped residuals from the mirror contaminated with porous W/O after 4 laser cleaning scans.

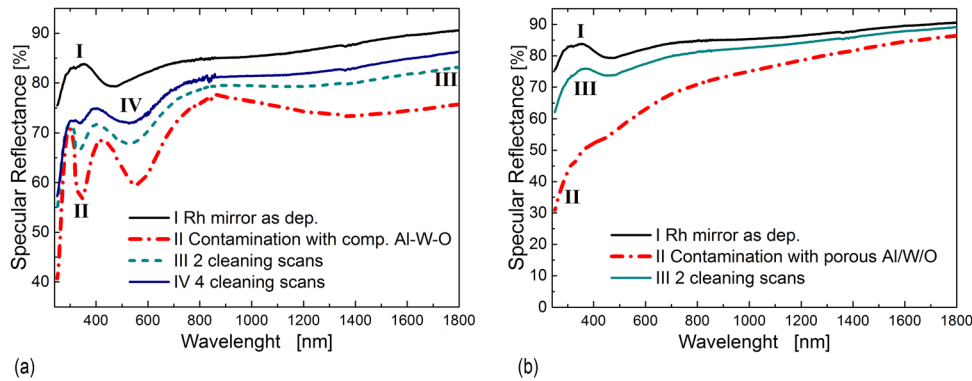


**Figure 13.** (a)  $R_{\text{spec}}$  of a Rh mirror before contamination (solid black), contaminated with compact Al/W/O (dashed red) after 2 laser cleaning scans (dashed light blue) and after 4 laser cleaning scans (solid dark blue). (b)  $R_{\text{spec}}$  of a Rh mirror before contamination (solid black), contaminated with porous Al/W/O (dashed red) and after 2 laser cleaning scans (solid light blue).

to which corresponds  $\lambda = 450$  nm). Diffuse reflectance (not shown) remained below 0.5 % in the whole spectrum.

SEM analysis (figure 12(a)) revealed that some regions of the sample were covered by residuals having a morphology very different from that of non-irradiated compact W/O (figure 1(a)). In addition, XPS analysis confirmed the presence of a  $\text{WO}_3$  layer on the mirror surface. The thickness of the residual layer can be estimated by evaluating its impact on the reflectance after the laser cleaning. Line IV (dashed green) in figure 11(a) shows the calculated reflectance of a semi-infinite Rh substrate with a 5 nm thick  $\text{WO}_3$  film on top. The refractive index of the film was estimated by means of ellipsometry measurements [37] performed on another (not irradiated) W/O contaminated Rh mirror using the Cauchy's model [37]. The excellent matching between the experimental and theoretical reflectance values confirms that the UV reflectance drop after the cleaning process should be attributed to a very thin  $\text{WO}_3$  layer that remained on the mirror surface. The measured  $R_{\text{diff}}$  (not shown) was below 1% in the whole wavelength range.

The specular reflectance of the mirror contaminated with porous W/O after 2 laser cleaning scans is shown in figure 11(b) (dashed light blue line, III). It is remarkably similar to the one obtained considering the cleaning of compact W/O contamination, despite the dramatic differences in contaminant morphology and optical properties.  $R_{\text{diff}}$  was below 1% in the whole 250–1800 nm range.

SEM microscopy revealed that some regions of the sample were covered by very small residuals, in form of nanometric

rod-shaped clusters (figure 12(b)). Also in this case, EDXS and XPS detected the presence of  $\text{WO}_3$ , which is likely responsible for the low UV reflectance.

After the first laser cleaning session, the same sample was cleaned again with two additional scans. The corresponding  $R_{\text{spec}}$  is plotted as the solid dark blue line (IV) in figure 11(b). By comparing dashed light blue and solid dark blue curves, we conclude that the additional cleaning cycles had a beneficial effect on the  $R_{\text{spec}}$  recovery in the UV region. The Rh coating appeared intact after the whole cleaning treatment (4 scans).

#### 4.3. Laser cleaning of Al/W/O contaminated mirrors

The mirror contaminated with the compact Al/W/O deposit was initially cleaned with 2 laser scans. After that, some macroscopic residuals were visible by naked eye. The corresponding  $R_{\text{spec}}$  is shown as the dashed light blue line (III) in figure 13(a). The same sample was irradiated again with two additional laser scans with the aim of increasing the cleaning efficacy. The specular reflectance after 4 cleaning cycles is reported as the solid dark blue line (IV) in figure 13(a). The loss in  $R_{\text{spec}}$  with respect to a pristine mirror varies from 5% ( $\lambda > 700$  nm) to 15% ( $\lambda = 250$  nm). The presence of an interference pattern is still visible.

SEM analysis (figure 14(a)) clearly shows the presence of regions in which the contaminant film is still integer and adherent to the Rh coating. On the other hand, there are some areas that seem totally cleaned. XPS surface analysis revealed the presence of Al (22 at.%) and O (42 at.%), together with a

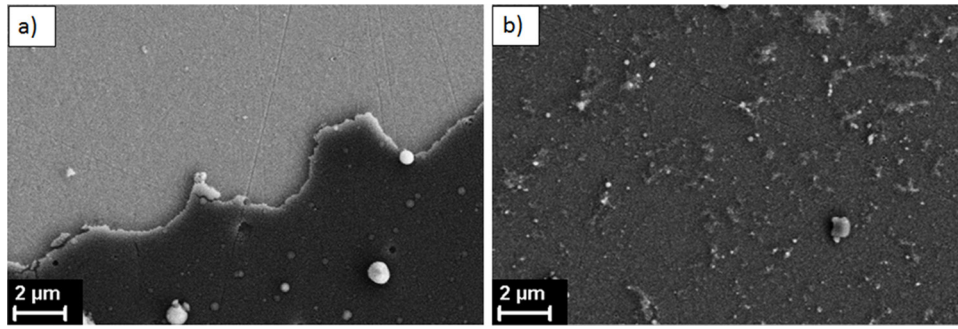


**Figure 14.** SEM top-view of: (a) compact Al/W/O residuals after 4 laser cleaning scans. Rh coating appears as the brighter region. (b) Porous Al/W/O residuals after 2 laser cleaning scans.

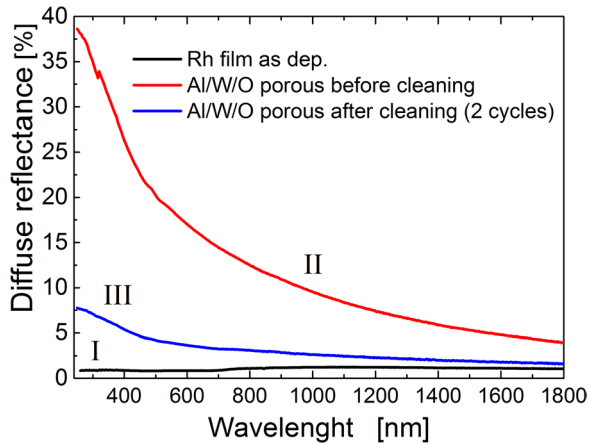


**Figure 15.**  $R_{\text{diff}}$  of a bare Rh mirror as deposited (I, black), after contamination with porous Al/W/O (II, red), after 2 scans of laser cleaning (III, blue).

clear Rh signal (35 at.%), which is indicative of a nearly complete contaminant removal.

As shown in figure 14(a), there is a sharp transition between the zone where the contaminant film is present and the cleaned one, as if the film underwent a brittle fracture. This fact suggests that laser induced thermo-mechanical stresses may have played a major role in contaminant removal. No damages of the Rh coating were observed.

The specular reflectance of the mirror contaminated with porous Al/W/O after 2 cleaning scans is shown in figure 13(b), solid light blue curve. The laser cleaning treatment ensured a satisfactory recovery of the mirror reflectance over the whole spectrum, ranging from 95% of the original value for  $\lambda > 400$  nm to 82% of the original value for  $\lambda = 250$  nm.

By comparing the diffuse reflectance before (figure 15, line II red) and after the laser cleaning (figure 15, line III blue), it is clear that the recovery in  $R_{\text{spec}}$  was essentially due to a decrease in  $R_{\text{diff}}$  as a consequence of the cleaning process.

SEM microscopy revealed that the Rh surface covered by Al/W/O porous structures was strongly decreased thanks to laser cleaning (figure 14(b)). As a consequence, the fraction of light randomly scattered from contaminant is diminished and the reflection from Rh film at the specular angle is increased.

This picture is confirmed by surface XPS analysis, which showed traces of Al (11 at.%) and a strong Rh signal (50 at.%) together with O (39 at.%). No damages of the mirror surface were observed.

## 5. Comparison and discussion

The experimental results discussed in sections 3 and 4 allowed us to address a comparison between plasma and laser cleaning techniques. The main criteria against which the comparison is made are:

- The recovery of specular reflectance, as a function of the contaminant characteristics and the spectral range.
- The integrity of the cleaned mirror.
- The time required to perform the treatment.

Because of inherent differences in the characteristics of the two spectrophotometers employed to measure the reflectance after the cleaning treatments, the cleaning results are compared in terms of  $R_{\text{spec}}$  recovery, defined as the ratio of pristine specular reflectance (i.e. before contamination) to the reflectance after cleaning, both measured with the same equipment. The  $R_{\text{spec}}$  recovery is shown in figures 16(a) and (b) for W/O and Al/W/O contaminants, respectively.

As far as compact contaminants were considered, plasma cleaning gave an excellent  $R_{\text{spec}}$  recovery.

In particular, in the case of compact W/O, the contaminant was completely removed, the mirror's surface was not altered by the plasma treatment, and the reflectance was slightly higher than the original value over the entire spectrum (figure 16(a), red solid line, I). In the case of compact Al/W/O contamination, the presence of some micrometric residuals and the roughening of the mirror surface can explain the incomplete  $R_{\text{spec}}$  recovery ( $\approx 80\%$ ) in the UV region (figure 16(b), red solid line, I). SEM analysis showed that the quality of the mirror surface was deteriorated by the plasma treatment (figure 8(b)). This degradation might evolve in a severe mirror damaging in the case of repeated plasma cleaning cycles.

Plasma cleaning failed to recover the mirror reflectance in the case of porous contaminants (figures 16(a) and (b), blue solid line, III). The failure was dramatic for porous Al/W/O, for which the Rh mirror optical properties were completely lost. For both W/O and Al/W/O contaminations, the cleaning process caused severe damage to the Rh coating while contaminants were still present on the surface (figures 6 and 10, respectively).

This issue is essentially related to the intrinsic non-homogeneity of the porous contaminants (in terms of thickness and morphology on the micro- and meso-scale), because of which the contaminant layer was removed faster in some areas than other, leading to early sputtering of the Rh mirror. In addition,



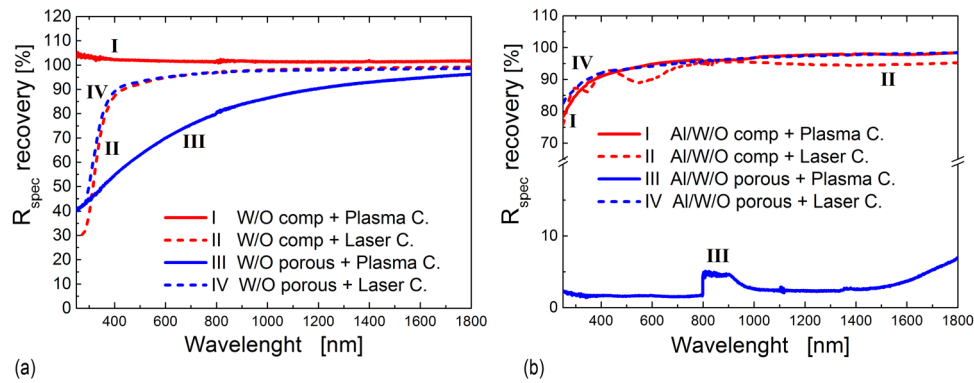


**Figure 16.** (a)  $R_{\text{spec}}$  recovery as a result of the plasma cleaning (solid lines) and laser cleaning (dashed lines) processes in the case of W/O contaminants. (b)  $R_{\text{spec}}$  recovery as a result of the plasma cleaning (solid lines) and laser cleaning (dashed lines) processes in the case of Al/W/O contaminants.

chemical modifications (i.e. reduction) induced by the plasma, that are favored in the porous materials because of their high surface-to-volume ratio, might have caused local variation of the contaminant sputtering yield. A potential solution to cope with these problems may be to change the composition of the sputtering gas and/or to reduce the energy of the ions. While it is not easy to predict the benefits of this strategy in the case of porous materials, it is almost sure that it would result in a slower sputtering rate, which implies a longer time to clean the same sample.

Since it is possible that thick, porous re-deposits will build-up on ITER FMs, one should consider carefully these issues in the design of FMs cleaning and deposition mitigation systems.

Laser cleaning proved to be much less sensitive to the contaminant morphology than plasma cleaning. For all the contaminations considered, the same laser cleaning procedure ensured a very good  $R_{\text{spec}}$  recovery (>90%) in the vis-NIR spectral range. This appears clearly by comparing the  $R_{\text{spec}}$  recovery achieved for porous and compact morphologies (red dashed line II and blue dashed line IV, respectively) in figure 16(a) (W/O contaminant) and figure 16(b) (Al/W/O contaminant). The robustness of the adopted laser cleaning procedure with respect to the contaminant characteristics (e.g. morphology and thickness) is especially valuable in the view of remote operations, since in principle one can perform the cleaning without characterizing in advance the status of the mirror's surface to be treated.

Considering the integrity of the mirrors, laser cleaning proved to be gentler than plasma cleaning, since it was possible to preserve the mirror integrity in all the cases by virtue of the proper selection of a sufficiently low ( $70 \text{ mJ cm}^{-2}$ ) laser fluence per pulse.

A major advantage of the laser cleaning technique is related to the shorter time required to perform the cleaning treatment. Considering for example the case of compact Al/W/O, 4 scans of UV laser pulses—which take less around 1 min each—gave a  $R_{\text{spec}}$  recovery similar to that obtained after 21 h of plasma exposure. In other words, in this specific case laser cleaning has been about 300 times faster than plasma cleaning. This feature could represent a major advantage in the frame of ITER development, since the laser cleaning of the mirrors could be performed *in situ* between the plasma discharges.

Nevertheless, it must also be remarked that the development of a laser delivery system suitable for working within the ITER environment would imply to face challenging technical and engineering aspects, such as the inclusion of suitable systems to protect the laser delivery optics from redeposition phenomena.

One should also consider that in a real reactor scenario a cleaning treatment would be probably required already for deposits thinner than the contaminants here employed. Since the plasma cleaning time linearly increases with the contaminant thickness, this fact will result in a reduced amount of time to plasma clean the mirrors.

For what concerns the reflectance recovery, the most critical issue in the case of laser cleaning is related to the presence of a very thin ( $\approx 5 \text{ nm}$ ) contaminant layer left on the cleaned surface which, in the case of W/O contamination, prevented the recovery of UV reflectance.

### 5.1. Combined plasmalaser cleaning approach

A natural way to exploit the best features of the two techniques would be a combined cleaning solution, in which laser cleaning is firstly adopted to quickly remove most of the contaminants with no limitations regarding their morphology. Then, a plasma cleaning session may follow, with the aim of removing the thin residual layer, if needed by the reflectance requirements of the diagnostic systems.

The feasibility of this solution was tested on the mirrors that were previously contaminated with compact and porous W/O and laser cleaned as described in section 3. The mirrors were subsequently exposed for 45 min each to the same plasma conditions described in section 4. For both samples, the XPS analysis performed after the final plasma cleaning session detected only Rh and O, indicating a complete removal of contaminants. The resulting specular reflectance is coincident with the pristine value, as can be appreciated in figure 17. In particular, the combined cleaning approach ensured a complete recovery of the mirror properties also in the UV region (where laser cleaning alone was not sufficient, see blue lines in figures 11(a) and (b)) and for porous contamination (very hard to treat by plasma cleaning alone). Furthermore, the time required for the combined cleaning is reduced by a factor of



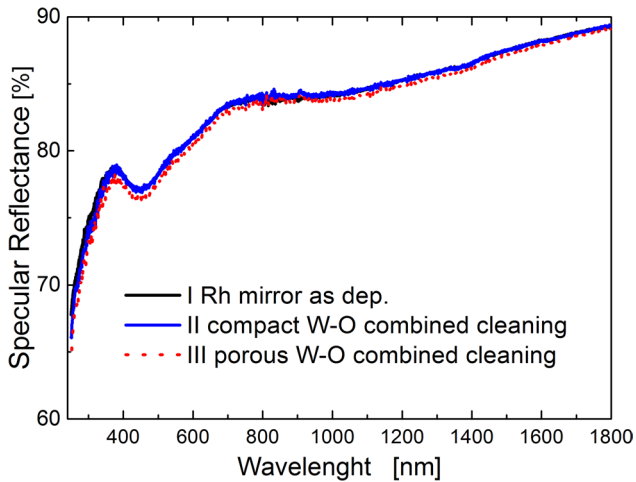


**Figure 17.**  $R_{\text{spec}}$  of a Rh mirror before contamination (I, black); contaminated with compact W/O after 2 laser cleaning scans and 45 min of plasma cleaning (II, blue); contaminated with porous W/O after 4 laser cleaning scans and 45 min of plasma cleaning (III, red).

4 (compact W/O) and a factor of 14 (porous W/O) if compared with plasma cleaning alone.

It is interesting to note that this solution exploits at best the robustness shown by the laser cleaning with respect to contaminant thickness and morphology. Indeed, no detailed characterization will be required before the laser cleaning treatment. In addition, given that the properties of the contaminant left after the laser treatment seem relatively independent from the original morphology, the need for extensive characterization before the plasma treatment is also reduced.

In spite of these advantages and the excellent cleaning results, the implementation of this combined cleaning solution in ITER diagnostic systems would be more challenging from a technical and engineering point of view. Whether the benefits offered by the combined approach will be worth facing these additional issues depends on a number of factors (mirror design choice, severity of the redeposition phenomena, diagnostic requirements, availability of alternative solutions) that are largely unknown at the moment. Additional investigations will be helpful in improving the efficacy of this cleaning solution, which may lead to a faster cleaning, and possibly to more relaxed requirements on the plasma and laser sources. This, in turn, might consent a simpler integration of the cleaning equipment in the ITER design.

## 6. Conclusions

In this work we presented an experimental comparison between plasma cleaning and laser cleaning, which are the two candidate cleaning techniques for the ITER first mirrors (FMs), in conditions potentially relevant for ITER scenarios. The two cleaning techniques were compared against three main criteria: the recovery of pristine mirror reflectance, the mirror integrity after cleaning, and the time required to perform the treatment.

We used 500 nm thick Rh films deposited by magnetron sputtering on a 1 inch wide S.S. substrate as test mirrors. The mirrors were contaminated with pulsed laser deposited W/O and Al/W/O materials having compact and porous morphology, aimed at reproducing the re-deposits expected on ITER FMs.

One set of mirrors was cleaned with RF plasma cleaning.  $\text{Ar}^+$  ions were accelerated by a self-bias of  $-300$  V. The relative variation of mirror reflectance was tracked by an *in situ* spectrophotometer in order to understand when to interrupt the plasma treatment.

The other set of mirrors was cleaned using laser cleaning with UV ( $\lambda = 266$  nm) laser pulses using a fast irradiation procedure which took about 1 min for a complete laser scan of the sample.

Considering that the laser damage threshold depends on the characteristics of the mirror to be cleaned, the laser fluence ( $70 \text{ mJ cm}^{-2}$  per pulse) was set in accordance with preliminary irradiation experiments on bare mirrors. Multiple scans (2 up to 4) were adopted to increase the reflectance recovery.

Plasma cleaning proved to be very effective in removing compact contaminations. This feature is particularly desirable in the case of contaminants that present a strong optical absorption in the spectral region of interest for the corresponding diagnostic system. Indeed, in the case of compact W/O,  $R_{\text{spec}}$  recovery was complete over the whole spectrum. On the other hand, for both porous W/O and porous Al/W/O plasma cleaning treatment produced macroscopic damages to the Rh coating and the reflectance was not recovered.

Laser cleaning is relatively insensitive to the contaminant morphology. A very good  $R_{\text{spec}}$  recovery (around 90%) in the vis–NIR spectral region was achieved for all the cleaned samples. In the case of W/O contaminants, UV reflectance recovery was more problematic due to presence of light absorbing residuals. Moreover, the laser cleaning strategy that we employed proved to be safer for the mirror integrity and significantly faster (up to 300 times with respect to the plasma cleaning procedure).

To conclude, we have shown that laser and plasma cleaning are characterized by different complementary features that can be suitably exploited for the cleaning of ITER FMs. In addition, we also demonstrated the potential benefits of a synergistic cleaning solution, which foresees laser cleaning as a fast and robust way to remove most of the contaminants and recover vis–NIR reflectance, followed by a plasma cleaning session to clear the mirror surface from residuals and recover also the UV reflectance. This strategy would be effective also in the case of porous materials, which seem very difficult to be cleaned by plasma alone.

On the other hand, the combined cleaning would require to integrate both a RF source and a laser delivery system in the same diagnostic set-up. Further investigations are required to assess the feasibility of this solution for the cleaning of ITER FMs.

## Acknowledgments

The authors wish to thank S. Perissinotto for his contribution to the reflectance measurements.

The authors would like to thank the Swiss Federal Office of Energy and the Federal Office for Education and Science for their financial support. This work was also supported by the Swiss National Foundation (SNF) and the Swiss Nanoscience Institute (SNI).

The research leading to these results has received funding from the European Research Council Consolidator Grant ENSURE (ERC-2014-CoG No. 647554).

## References

- [1] Walsh M. et al 2011 *IEEE/NPSS 24th Symp. on Fusion Engineering (Chicago, IL, USA, 26–30 June 2011)* S03A-1 (<http://ieeexplore.ieee.org/document/6052210/>)
- [2] Mukhin E.E. et al 2012 *Nucl. Fusion* **52** 013017–26
- [3] Mukhin E.E. et al 2009 *Nucl. Fusion* **49** 085032
- [4] Arkhipov I. et al 2013 *J. Nucl. Mater.* **438** S1160–3
- [5] Yan R. et al 2015 *J. Nucl. Mater.* **463** 948–51
- [6] Rogov A.V. et al 2015 *Instrum. Exp. Tech.* **58** 161–6
- [7] Razdobarin A.G. et al 2015 *Nucl. Fusion* **55** 093022
- [8] Moser L. et al 2015 *J. Nucl. Mater.* **463** 940–3
- [9] Moser L. et al 2015 *Nucl. Fusion* **55** 063020
- [10] Moser L. et al 2016 *Phys. Scr.* **T167** 014069
- [11] Widdowson A. et al 2011 *J. Nucl. Mater.* **415** S1199–202
- [12] Zhou Y. et al 2013 *J. Nucl. Mater.* **415** S1206
- [13] Skinner C.H. et al 2013 *Fusion Sci. Technol.* **64** 1
- [14] Wisse M. et al 2014 *Fusion Eng. Des.* **89** 122–30
- [15] Uccello A. et al 2013 *Fus. Eng. Des.* **88** 1347–51
- [16] Maffini A. et al 2015 *J. Nucl. Mater.* **463** 944–7
- [17] Maffini A. et al 2016 *Nucl. Fusion* **56** 086008
- [18] Mertens Ph. et al 2015 *Fusion Eng. Des.* **96–7** 129–13
- [19] Litnovsky A. et al 2015 *Nucl. Fusion* **55** 093015
- [20] Kane D. 2006 *Laser Cleaning II* (Singapore: World Scientific)
- [21] Hernandez C. et al 2010 *IEEE Trans. Plasma Sci.* **38** 3
- [22] Alfier A. et al 2010 *J. Phys.: Conf. Ser.* **227** 012036–9
- [23] Marot L. et al 2007 *Rev. Sci. Instrum.* **78** 103507–13
- [24] Marot L. et al 2008 *Surf. Coat. Technol.* **202** 2837
- [25] Rubel M. et al 2011 *Phys. Scr.* **T145** 014070–5
- [26] Ivanova D. et al 2014 *Phys. Scr.* **T159** 014011
- [27] Litnovsky A. et al 2013 *Nucl. Fusion* **53** 073033
- [28] Marot L. et al 2015 *J. Coat. Sci. Technol.* **2** 72–8
- [29] Uccello A. et al 2013 *J. Nucl. Mater.* **432** 261–5
- [30] Palik E.D. 1985 *Handbook of Optical Constants of Solids* (New York: Academic)
- [31] Marot L. et al 2013 *Fusion Eng. Des.* **88** 1718–21
- [32] Rasinski M. et al 2011 *Fusion Eng. Des.* **86** 1753
- [33] Dellasega D. et al 2012 *J. Appl. Phys.* **112** 084328
- [34] Maffini A. 2015 Laser cleaning of diagnostic first mirrors for nuclear fusion machines *PhD Thesis* Politecnico di Milano (<http://hdl.handle.net/10589/114506>)
- [35] Marot L. et al 2008 *Surf. Sci.* **602** 3375–80
- [36] Wisse M. et al 2012 *Rev. Sci. Instrum.* **83** 013509
- [37] Rapp J. et al 2009 *Phys. Scr.* **T138** 014067